Roles of pH, ionic strength, and sulfate in the aqueous nitrate-mediated photooxidation of green leaf volatiles

Yuting Lyu[1,2], Taekyu Joo[3], Ruihan Ma[1], Mark Kristan Espejo Cabello[1,2], Tianye Zhou[1], Shun Yeung[1], Cheuk Ki Wong[1], Yifang Gu[1], Yiming Qin[1], Theodora Nah[1,2]*

[1]School of Energy and Environment, City University of Hong Kong, Hong Kong SAR, China
[2]State Key Laboratory of Marine Pollution, City University of Hong Kong, Hong Kong SAR, China
[3]Department of Earth and Environmental Sciences, Korea University, Seoul, South Korea

Correspondence to: Theodora Nah (theodora.nah@cityu.edu.hk)

Abstract. Biotic and abiotic stresses can lead to terrestrial green plants releasing green leaf volatiles (GLVs), which can partition into atmospheric aqueous phases where they can undergo oxidation to form aqueous secondary organic aerosols (aqSOA). Anthropogenic emission changes have resulted in nitrate becoming an increasingly important component of atmospheric aqueous phases, which has significant implications for aqSOA formation since nitrate photolysis produces oxidants. Nevertheless, sulfate remains the main inorganic aqueous component in most regions, and thus controls the pH and ionic strength of atmospheric aqueous phases. We report results from laboratory investigations of the effects of pH, ionic strength, and sulfate on the reaction kinetics and aqSOA formation of the aqueous nitrate-mediated photooxidation of four GLVs, *cis*-3-hexen-1-ol, *trans*-2-hexen-1-ol, *trans*-2-penten-1-ol, and 2-methyl-3-buten-2-ol. Our results showed that the aqueous reaction medium conditions, i.e., dilute cloud/fog vs. concentrated aqueous aerosol conditions, governed the effects that pH, ionic strength, and sulfate have on the GLV degradation rates and aqSOA mass yields. Most notably, reactions initiated by sulfate photolysis will have significant effects on the GLV degradation rates and aqSOA mass yields in aqueous aerosols, but not in cloud/fog droplets. In addition to providing new insights into aqSOA formation from the aqueous reactions of GLVs in regions with substantial concentrations of nitrate in cloud, fog, and aqueous aerosols, this study highlights how nitrate and sulfate photochemistries can couple together to influence the reactions of water-soluble organic compounds and their aqSOA formation in aqueous aerosols, which have implications for our evaluations of aqueous organic aerosol lifetimes and composition.

1 Introduction

Biogenic volatile organic compounds (BVOCs) contribute more than 80 % of the global volatile organic compound (VOC) emissions (Guenther et al., 2012; Sindelarova et al., 2014). Isoprene and monoterpenes comprise more than half of the total annual BVOC emissions (Sindelarova et al., 2014). Since green leaf volatiles (GLVs) comprise a comparatively smaller fraction of total BOVCs, their chemical processes have received far less attention compared to isoprene and monoterpene. GLVs are C_5 to C_6 unsaturated organic compounds with aldehyde, alcohol, or ester functional groups (Sarang et al., 2021a).

GLVs are emitted during the decomposition of C_{18} polyunsaturated fatty acids in leaves when vegetation is exposed to herbivores, pathogens, or harsh weather conditions (Ameye et al., 2018; Matsui and Engelberth, 2022b; Silva et al., 2021). They are also emitted by cyanobacteria and algae during bloom events (García-Plazaola et al., 2017). GLVs have the potential to contribute substantially to the local secondary organic aerosol (SOA) budget due to their increased emissions when vegetation is subjected to biotic and abiotic stresses. A previous study reported that GLV emissions from Amazon tropical forests increased significantly in the afternoon due to the plants' response to rising temperatures, whereas isoprene and monoterpene emissions decreased (Jardine et al., 2015). Global GLV emissions will potentially increase in the future due to climate change and the increasing use of new fumigation-based agricultural, horticultural, and forestry practices (Cofer et al., 2018; Matsui and Engelberth, 2022a; Su et al., 2020). Thus, GLVs may play increasingly important roles in atmospheric chemistry, which necessitates increasing our knowledge of their multiphase reactions and SOA formation.

GLVs can be oxidized by ozone and hydroxyl radicals (·OH) in the gas phase to produce low volatility products, with reported SOA mass yields ranging from 0.7 to 20 % (Hamilton et al., 2009; Harvey et al., 2014; Jaoui et al., 2012; Mentel et al., 2013). Due to their moderately high water solubilities, GLVs can dissolve into atmospheric aqueous phases (e.g., aqueous aerosols, cloud and fog droplets), where they can be oxidized by aqueous oxidants such as ·OH, sulfate anion radicals ($SO_4^{·-}$), nitrate radicals ($NO_3·$), triplet organic excited states ($^3C^*$), and singlet oxygen ($^1O_2^*$) (Richards-Henderson et al., 2014; Richards-Henderson et al., 2015; Sarang et al., 2021a; Sarang et al., 2021b; Sarang et al., 2023). Higher quantities of low volatility products are formed from aqueous reactions compared to gas-phase reactions, with previous studies reporting aqueous SOA (aqSOA) mass yields as high as 88 % though this will depend on the GLV and the aqueous oxidant (Richards-Henderson et al., 2014; Richards-Henderson et al., 2015). However, these previous studies were mostly conducted under dilute aqueous conditions mimicking aqueous cloud/fog droplets. Differences in the physicochemical properties of the aqueous reaction medium will impact reaction rates in cloud/fog droplets vs. aqueous aerosols (Herrmann et al., 2015), but little is currently known about the aqueous oxidation of GLVs under more concentrated aqueous aerosol-like conditions.

The liquid water concentrations (LWC) of cloud and fog droplets typically fall in the range of 0.05 to 0.5 g/m^3 (Achtert et al., 2020; Kim et al., 2022; Korolev et al., 2007), whereas the LWC of aqueous aerosols fall in the range of 10^{-7} to 10^{-3} g/m^3 (Herrmann et al., 2015). Thus, the concentrations of dissolved organic and inorganic compounds are higher in aqueous aerosols, with their dry masses close to the liquid water mass (Nguyen et al., 2016). The concentrations of inorganic ions, particularly nitrate and sulfate, primarily govern the acidities and ionic strengths of atmospheric aqueous phases. Cloud and fog droplets (pH 2 to 7) are generally less acidic than aqueous aerosols (pH 0 to 5) due to the more frequent ammonia dissolution and higher buffering capacities of cloud and fog droplets (Pye et al., 2020; Tilgner et al., 2021). The ionic strengths of atmospheric aqueous phases span a large range (10^{-5} M to 10^0 M), with the ionic strengths of aqueous aerosols being several orders of magnitude higher than those of cloud and fog droplets (Herrmann et al., 2015; Tilgner et al., 2021). Under the high ionic strength conditions in aqueous aerosols, substantial ion association occurs, which will affect the activity coefficients of organic compounds, resulting in reactions occurring under non-ideal conditions (Herrmann, 2003). Previous studies have

65 reported that ionic strength significantly affect the aqueous reactions of some organic compounds and subsequent product formation (Herrmann, 2003; Mekic et al., 2018a; Mekic et al., 2018b; Mekic and Gligorovski, 2021; Zhou et al., 2019). In addition to contributing to the acidity and ionic strength of atmospheric aqueous phases, inorganic nitrate and sulfate can undergo photolysis to produce various reactive species that react with organic compounds. The tropospheric irradiation of nitrate in atmospheric aqueous phases is known to produce aqueous reactive species such as ·OH, nitric oxide radicals (NO·),

70 and nitrogen dioxide radicals (NO$_2$·) that can react with organic compounds (Mack and Bolton, 1999; Gen et al., 2022). Even though a recent study reported that sulfur-containing radicals (e.g., SO$_4^{-}$) are formed during the tropospheric irradiation of aqueous sulfate aerosols (Cope et al., 2022), the mechanisms behind their formation are still not well understood. While nitrate is increasingly important in regions with large reductions in sulfur dioxide emissions and/or with high ammonia emissions (Heald et al., 2012; Schaap et al., 2004; West et al., 1999), sulfate remains the dominant inorganic constituent of atmospheric

75 aqueous phases in most regions (Bianco et al., 2020). At present, little is known about how inorganic nitrate and sulfate salts influence the aqueous oxidation of GLVs.

In this study, we investigated the nitrate-mediated photooxidation of four GLVs, *cis*-3-hexen-1-ol, *trans*-2-hexen-1-ol, *trans*-2-penten-1-ol, and 2-methyl-3-buten-2-ol (Figure 1), under cloud/fog-like and aqueous aerosol-like conditions. These four GLVs, which are amongst some of the more abundant GLVs, have Henry's law constants between 60 to 120 M atm^{-1}

80 (Sander, 2023; Sarang et al., 2021a). Thus, they can partition efficiently into cloud/fog droplets and moderately into aqueous aerosols (Figure S1). We investigated the effects of pH, ionic strength, and sulfate on the reaction kinetics and aqSOA mass yields under cloud/fog-like and aqueous aerosol-like conditions. Results from this study provide new insights into the aqueous photooxidation of GLVs in regions with substantial levels of nitrate in cloud and fog droplets and aqueous aerosols, and more generally, how sulfate photochemistry impacts the aqueous nitrate-mediated photooxidation of other water-soluble organic

85 compounds.
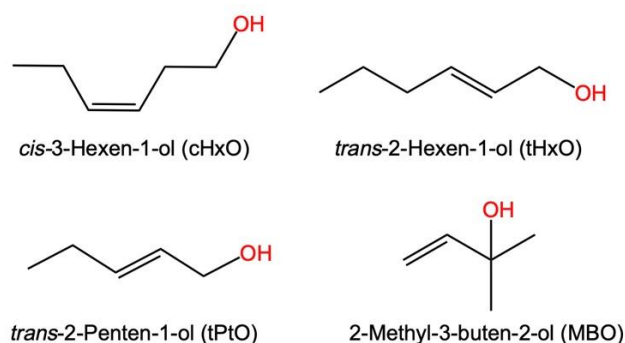
Figure 1. The four model GLVs used in this study.

2 Methods

2.1 Chemicals and Solutions

All the chemicals were used as received. *cis*-3-Hexen-1-ol (cHxO, 98 %), *trans*-2-hexen-1-ol (tHxO, 96 %), 2-methyl-3-buten-2-ol (MBO, 97 %), benzoic acid (BA, 99.5 %) and p-hydroxybenzoic acid (pHBA, 99 %) were purchased from J&K Scientific. *Trans*-2-penten-1-ol (tPtO, ≥ 95 %) was purchased from Aladdin Scientific. Ammonium nitrate (NH_4NO_3, ≥ 95 %) and ammonium sulfate ((NH_4)$_2SO_4$, 99+ %) was purchased from Fisher Scientific. Sulfuric acid (H_2SO_4, 95 %) was purchased from VWR Chemicals BDH®. Milli-Q ultrapure water (18.2 MΩ cm) was used to prepare all solutions.

Table 1 shows the concentrations of solutions used to simulate cloud/fog-like and aqueous aerosol-like conditions in photochemistry experiments. The same nitrate/GLV molar concentration ratio (i.e., 2.5:1) was used for both cloud/fog-like and aqueous aerosol-like conditions. The concentrations of the GLVs and NH_4NO_3 were set to be 100 times higher for the aqueous aerosol-like conditions than the cloud/fog-like conditions. The nitrate concentration (i.e., 250 µM) used for cloud/fog-like conditions is close to those measured in cloud water in Hong Kong (average of 238 µM) (Li et al., 2020) and is within the global range for nitrate in continental cloud water (Bianco et al., 2020). Even though the nitrate concentration in aqueous aerosols could reach molar levels (Bzdek et al., 2020), we used 25 mM of NH_4NO_3 in experiments that simulate aerosol-like conditions to maintain the same nitrate/GLV molar concentration ratio as in experiments that simulate cloud/fog-like conditions. The pH of unbuffered solutions (no addition of H_2SO_4) were close to 5, and it was selected as the higher bound to study the pH effects on the nitrate-mediated photooxidation of GLVs. The lower bound of pH was set to 3 through the addition of H_2SO_4. (NH_4)$_2SO_4$ was added into the solutions to control the sulfate concentrations in and ionic strengths of the solutions. Since the acid dissociation constant (pK_a) for $HSO_4^- \leftrightarrow H^+ + SO_4^{2-}$ is around 2.0 at 25 °C (Dickson et al., 1990), SO_4^{2-} are expected to be the dominant species even at the lower bound of pH 3. The pH (i.e., pH 3 vs. 5, Table 1) used in this study fall within the ranges for cloud and fog droplets and aqueous aerosols (Herrmann et al., 2015; Pye et al., 2020; Tilgner et al., 2021). The ionic strengths (I_{total}) of the solutions were calculated using the following equation:

$$I_{total} = \frac{1}{2} \times \sum_{i=1}^{i=n} c_i z_i \tag{1}$$

where c_i and z_i are the concentration (M) and charge, respectively, of inorganic ion i for H^+, NH_4^+, NO_3^-, and SO_4^{2-}. The ionic strengths used in this study, i.e., 0.002 M vs. 0.02 M for cloud/fog-like conditions and 0.5 M vs. 3.3 M for aqueous aerosol-like conditions (Table 1), fall within the ranges for ionic strengths for clouds/fog droplets and continental aerosols (Herrmann et al., 2015). Only the addition of tPto and tHxO had significant effects on the molar absorptivity of NH_4NO_3 (Figure S2b), enhancing the peak molar absorptivity of NH_4NO_3 by approximately 1.3 and 1.5 times, respectively.

Table 1. Concentrations of GLVs, NH$_4$NO$_3$, H$_2$SO$_4$, (NH$_4$)$_2$SO$_4$, the pH, and I_{total} of solutions used to simulate cloud/fog-like and aqueous aerosol-like conditions in photochemistry experiments.

Simulated condition	[GLV] (mM)	[NH$_4$NO$_3$] (mM)	[H$_2$SO$_4$] (mM)	pH	[(NH$_4$)$_2$SO$_4$] (mM)	I_{total} (M)
Cloud/fog-like	0.1	0.25	0.5	3	0.135	0.002
					6.135	0.02
			0	5	0.583	0.002
					6.580	0.02
Aqueous aerosol-like	10	25	0.5	3	158	0.5
					1085	3.3
			0	5	158	0.5
					1085	3.3

2.2 Photochemistry Experiments

The solutions were placed into open cylindrical quartz tubes (1.2 cm inner diameter), which were placed on a rotating sample holder located in the middle of a photoreactor (Rayonet RPR-200, Southern New England UV Co.) surrounded by UVB lamps (RPR-3000Å, Southern New England UV Co.). The photon flux in the photoreactor ranged from 250 to 400 nm and peaked at 311 nm (Figure S2a). The temperature inside the photoreactor during experiments was maintained at around 30 °C by a cooling fan located at the bottom of the photoreactor. The volume of each quartz tube was around 15 mL. The quartz tubes were filled with 10 mL and 1 mL of solutions during experiments simulating cloud/fog-like and aqueous aerosol-like conditions, respectively. Aliquots of 1 mL and 0.1 mL were extracted from the illuminated solutions at different reaction times for offline chemical analysis during experiments simulating cloud/fog-like and aqueous aerosol-like conditions, respectively. For experiments simulating aqueous aerosol-like conditions, the extracted volume (0.1 mL) was diluted with Milli-Q ultrapure water by a factor of 10 prior to chemical analysis to ensure that the measured signals stayed within the linear detection range of detector. The decays of the GLVs were measured using an ultrahigh-performance liquid chromatography coupled to a photodiode array detector (UPLC-PDA, H-class, Waters). A Kinetex Polar C18 column (2.6 μm, 100 × 2.1 mm) equipped with a security guard and Polar C18 pre-column was used for the measurement of the four GLVs. An isocratic elution program set to 0.3 mL/min was used. The mobile phases of water and acetonitrile were run at a ratio of 80:20 for cHxO, tHxO, and MBO, and at a ratio of 85:15 for tPtO. The detection wavelengths were set to 240 nm for MBO, and 210 nm for the other three

GLVs. All the experiments and measurements were performed three times. All the decays of the GLVs followed apparent first order reaction kinetics reasonably well (Figures S3 and S4), thus they were fitted with the following equation:

$$\ln\left(\frac{[GLV]_t}{[GLV]_0}\right) = -k_{obs}t \tag{2}$$

where k_{obs} is the pseudo-first order rate obtained from the exponential fit to the photodegradation of the GLV, and $[GLV]_t$ and $[GLV]_0$ are the concentrations of individual GLV measured by UPLC-PDA at illumination times t and 0, respectively.

No loss in GLVs was observed in dark control experiments conducted in the absence and presence of nitrate and sulfate. During illumination in control experiments conducted in the absence of nitrate and sulfate ("light only" experiments), only MBO had significant loss under cloud/fog-like conditions, whereas all four GLVs had significant losses under aqueous aerosol-like conditions (Figures S3 and S4). The four GLVs were not expected to undergo direct photolysis as they do not absorb light significantly at wavelengths larger than 280 nm (Richards-Henderson et al., 2014; Sarang et al., 2021a), as demonstrated in Figures S5 and S6. Thus, the observed losses under illumination in control experiments conducted in the absence of nitrate and sulfate could be due to evaporation, with MBO having the largest losses due to its higher vapor pressure (3.08×10^{-2} atm) compared to the other three GLVs (cHxO: 1.23×10^{-3} atm, tHxO: 1.20×10^{-3} atm, and tPtO: 3.46×10^{-3} atm) based on estimations using EPI Suite™ (U.S. EPA, 2024). The k_{obs} values measured for the GLVs decays in nitrate-mediated photooxidation experiments were subsequently corrected by subtracting the loss rates from control experiments conducted in the absence of nitrate and sulfate ("light only" experiments).

To gain insights into how concentration, pH, and ionic strength affect ·OH formation during nitrate-mediated photooxidation, a separate set of experiments (i.e., GLVs were not present in the solutions) using BA (10 μM) as the ·OH probe compound was conducted to estimate the steady-state concentrations of ·OH ([·OH]$_{ss}$) using the same methodology as our past studies (Lyu et al., 2023; Yang et al., 2021; Yang et al., 2023). p-HBA, which is formed from the reaction of ·OH with BA ($k_{BA+OH} = 5.9 \times 10^9$ M^{-1} s^{-1} (Herrmann et al., 2010)) at a yield of 0.17 (Anastasio and Mcgregor, 2001), was measured in these experiments using an ultra-high performance liquid chromatography system (1290 system, Agilent) coupled to a high-resolution quadrupole-time-of-flight mass spectrometer (X500R QTOF MS/MS, Sciex) (UPLC-MS) equipped with an electrospray ionization (ESI) source that was operated in negative mode (Section S1). Solid phase extraction (SPE) using two different types of SPE cartridges (Oasis MAX, 60 mg, 3 cc, 60 μm, Waters; Bond PPL Elut, 200 mg, 3 mL, 125 μm, Agilent) was performed to remove inorganic salts from samples before UPLC-MS analysis. The estimated [·OH]$_{ss}$ values for the cloud/fog-like and aqueous aerosol-like conditions are shown in Figure S7.

2.3 AqSOA Mass Yields

Aerosol mass spectrometry was used to measure the aqSOA mass yields of the four GLVs. Aliquots of 10 mL and 1 mL were extracted from the illuminated solutions at one GLV lifetime (i.e., $\tau = \frac{1}{k_{obs}}$, when 37 % of the initial concentration of the GLV remained) in experiments simulating cloud/fog-like and aqueous aerosol-like conditions, respectively (Tables S2 and S3). The time points equivalent to one GLV lifetime were determined from the forementioned kinetic experiments. For experiments simulating aqueous aerosol-like conditions, the extracted volume (1 mL) was diluted with Milli-Q ultrapure water by a factor of 300 prior to aerosol mass spectrometry analysis to ensure that the measured signals stayed within the linear detection range of detector. Each sample solution was injected at 10 mL/h by a syringe pump (Model 100, KD Scientific) into an aerosol generation system (Model 9200, Brechtel Manufacturing Incorporated), which aerosolized the solution. The atomizer system used nitrogen gas (99.999 % purity) as the carrier gas at a flow rate of 4.5 L/min. The aerosols generated were passed through an inline dryer before entering a time-of-flight aerosol chemical speciation monitor (ACSM, Aerodyne Research Inc.). All the experiments and measurements were performed three times.

The aqSOA mass yield (Y_{SOA}) was calculated using the following equation (Jiang et al., 2023; Ma et al., 2021):

$$Y_{SOA} = \frac{Organic\ mass\ increased}{GLV\ mass\ decreased} = \frac{[Org]_\tau - [Org]_0}{[GLV]_0 - [GLV]_\tau}$$

$$= \frac{[Org]_{ACSM,\tau} \times \frac{[SO_4^{2-}]_\tau}{[SO_4^{2-}]_{ACSM,\tau}} - [Org]_{ACSM,0} \times \frac{[SO_4^{2-}]_0}{[SO_4^{2-}]_{ACSM,0}}}{(1 - 0.37) \times [GLV]_0} \tag{3}$$

where the [Org], [GLV], and [SO_4^{2-}] were the concentrations of organics, the GLV of interest, and sulfate, respectively. The terms with subscript of ACSM indicate the mass concentrations (in mg/L) of aerosols measured by the ACSM, which is different from the molar concentrations (mol/L) of solutions which do not have the ACSM subscripts. The subscripts τ and 0 indicate the sample solutions obtained at one GLV lifetime (Tables S2 and S3) and before illumination, respectively. The concentrations of sulfate in the solutions before and after illumination were assumed to be the same (i.e., $[SO_4^{2-}]_\tau = [SO_4^{2-}]_0$). The concentration of sulfate in each sample solution (Table 1) was used as the internal standard to scale the concentrations of organics measured by ACSM to those of the solutions. This is because sulfate is non-refractory and is expected to be collected and quantified by the ACSM, which had a capture vaporizer with a collection efficiency of 1 (Daellenbach et al., 2016; Xu et al., 2018; Joo et al., 2021). Additionally, the sulfate and organic composition in the atomized aerosols are expected to be internally mixed together (Ma et al., 2021).

3 Results and Discussion

3.1 Cloud/fog-like Conditions

3.1.1 Reaction Kinetics

The concentrations of the four GLVs decreased upon irradiation in the presence of nitrate and sulfate. In contrast to
MBO, no decays were observed for cHxO, tHxO, and tPtO when only sulfate was present (but not nitrate) in the solutions. In
the absence of nitrate, the MBO decay rates obtained in the absence and presence of sulfate were similar. The MBO decay in
the absence of nitrate could be due to MBO evaporation since it has a higher vapor pressure than the other three GLVs. Overall,
these results indicated that sulfate has an insignificant effect on the kinetics of the four GLVs under cloud/fog-like conditions.

Figure 2 shows the k_{obs} values for the four GLVs upon irradiation in the presence of nitrate at different pH (i.e., 3 vs.
5) and ionic strength (i.e., 0.002 M vs. 0.02 M). Separate experiments performed in the absence of GLVs and using BA as the
·OH probe compound showed that the estimated $[·OH]_{ss}$ values decreased with pH under these cloud/fog-like conditions
(Figure S7a), consistent with results reported by Lyu et al. (2023). The k_{obs} values for the four GLVs were on the orders of 10^{-5} to 10^{-4} s^{-1} for the four GLVs. The decays in the four GLVs upon irradiation in the presence of nitrate were due to the reactions
of the GLVs with reactive species produced from nitrate photolysis such as ·OH, NO·, and NO$_2$· (Table S1). Even though
approximately equal quantities of ·OH and NO$_2$· are produced during nitrate photolysis (Chen et al., 2019; Zhang et al., 2021),
the typical reactivities of NO$_2$· are 2 to 5 orders of magnitude lower than ·OH (Ford et al., 2002; Chen et al., 2019; Zhang et
al., 2021). Other reactive species produced during nitrate photolysis (e.g., hydroperoxide radicals (HO$_2$·) and superoxide ions
(O$_2$·$^-$)) are also expected to have lower reactivities compared to ·OH (Bielski et al., 1985; Mack and Bolton, 1999). Reaction
with ·OH was also shown to be the main contributor to the reaction kinetics of other non-photolyzable organic compounds
(e.g., formic acid, glycolic acid) during aqueous nitrate-mediated photooxidation (Lyu et al., 2023). While it is possible that
sulfur-containing radicals and other reactive species were formed from the photolysis of (NH$_4$)$_2$SO$_4$ (Table S4), their effects
on k_{obs} are small due to their low concentrations under diluted cloud/fog-like conditions (Cope et al., 2022). Additionally, the
k_{obs} values measured under illumination in control experiments conducted in the presence of sulfate only were not statistically
different ($p > 0.05$) from the k_{obs} values measured under illumination in control experiments conducted in the absence of nitrate
and sulfate ("light only" experiments). Thus, the decays of the GLVs were likely governed mostly by their reactions with ·OH,
though minor contributions from their reactions with reactive species other than ·OH cannot be discounted.
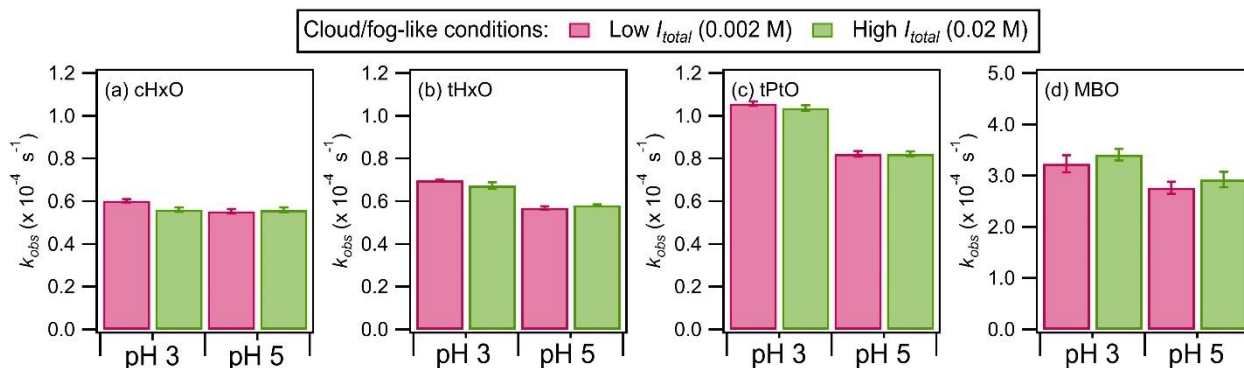
Figure 2. The k_{obs} values for the four GLVs during nitrate-mediated photooxidation under cloud/fog-like conditions (Table 1). The error bars represent one standard deviation originating from triplicate experiments and measurements. Statistical analyses (student's *t* test) on the differences in the k_{obs} values are presented in Tables S6 to S9.

Under the same ionic strength conditions, the four GLVs had higher k_{obs} at pH 3 than at pH 5, though the pH-dependent trends for cHxO at I_{total} = 0.002 M and 0.02 M were statistically insignificant ($p > 0.05$) (Table S5). The four GLVs do not have acidic H atoms, thus they do not undergo acid dissociation to form different relative abundances of deprotonated and neutral forms with different reactivities at different pH. Additionally, Richard-Henderson et al. (2014) showed that the ·OH rate constants for many GLVs do not depend on pH. Hence, the pH-dependent k_{obs} trends in Figure 2 were due to the pH-dependent formation of ·OH (Figure S7) and other reactive species from nitrate photolysis. HNO$_2$, whose production from nitrate photolysis is favored over NO$_2^-$ production at pH $\leq$ 3.5 (Marussi and Vione, 2021), has a higher quantum yield for ·OH formation than NO$_2^-$ in the near-UV region (Arakaki et al., 1999; Marussi and Vione, 2021). Thus, the formation rates and concentrations of ·OH produced at pH 3 are higher than at pH 5, which would explain the higher k_{obs} at pH 3. There were no statistically significant differences in the k_{obs} values for I_{total} of 0.002 M vs. 0.02 M under the same pH conditions for the four GLVs ($p > 0.05$). This indicated that ionic strength (and sulfate) has an insignificant effect on the reaction kinetics of the four GLVs under cloud/fog-like conditions. Overall, only pH impacted the reaction kinetics of the four GLVs significantly under cloud/fog-like conditions.

3.1.2 AqSOA Mass Yields

Figure 3 shows the Y_{SOA} values for the four GLVs measured at one GLV lifetime during irradiation in the presence of nitrate at different pH (i.e., 3 vs. 5) and ionic strength (i.e., 0.002 M vs. 0.02 M). The measured Y_{SOA} values (0 to 53 %) are in line with the range of Y_{SOA} values (10 to 88 %) measured by Richards-Henderson et al. (2014) for five GLVs (including cHxO and MBO) at one GLV lifetime in their reactions with ·OH generated from H$_2$O$_2$ photolysis under cloud/fog-like conditions.
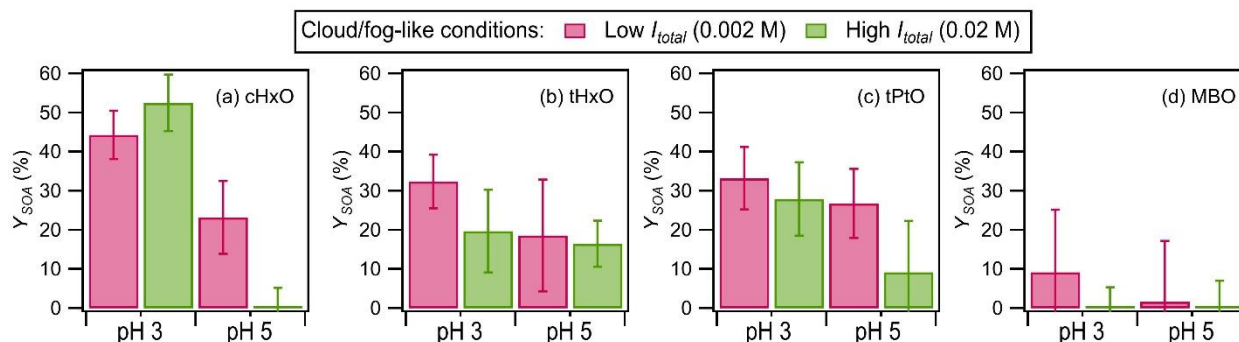
Figure 3. Y_{SOA} values for the four GLVs at one GLV lifetime during nitrate-mediated photooxidation under cloud/fog-like conditions. The error bars represent one standard deviation originating from triplicate experiments and measurements, and include errors propagated from the standard deviations of the sulfate concentrations measured by ACSM. The ACSM-measured organic signals for cHxO at pH 5 and I_{total} = 0.02 M, and for MBO at pH 3 and 5 at I_{total} = 0.02 M, and at pH 5 at I_{total} = 0.002 M were very low, resulting in close to zero organic concentrations and Y_{SOA} values. Therefore, there was essentially no formation of low volatility products from these three experiments, and the Y_{SOA} values were essentially zero. Statistical analyses (student's t test) on the differences in the Y_{SOA} values are presented in Tables S10 to S13.

Given the high reactivity of ·OH, reactions of the GLVs with ·OH are expected to produce products that contribute substantially to aqSOA formation. However, we cannot discount the possibility that other reactive species produced from nitrate/sulfate photolysis (Tables S1 and S4) also contributed to aqSOA formation. The reaction of ·OH with the GLV is expected to occur either by ·OH addition to the C=C bonds to form hydroxy alkyl radicals, or by H abstraction from the C-H or O-H bonds to form alkyl radicals (Figures S8 and S9). The H bond dissociation energies at the CH_2, CH_3, and OH groups are around 393, 419, and 436 kJ mol^{-1}, respectively (Benson, 1976). H abstraction is expected to occur preferentially at C-H sites α to the OH group (Cooper et al., 2009; Sarang et al., 2023). The hydroxy alkyl radicals and alkyl radicals subsequently react with O_2 to form peroxy radicals (RO_2·), which then react with other RO_2· to form either higher molecular weight carbonyls and alcohols or alkoxyl radicals (RO·). RO· can undergo fragmentation reactions to form lower molecular weight compounds. Even though they are not shown in our proposed reaction mechanisms in Figures S8 and S9, bimolecular combination reactions involving RO_2· and RO· (e.g., RO_2· + RO_2·) that form oligomers could have also contributed to aqSOA formation.

Attempts to identify prominent low volatility products (and their formation pathways) that contributed to aqSOA using liquid chromatography-mass spectrometry were unsuccessful due to the presence of large quantities of inorganic salts in the samples, which negatively impacted the ionization efficiencies of the products. Nevertheless, low volatility products from both the ·OH addition and H abstraction channels likely contributed to aqSOA formation for the four GLVs. Sarang et al. (2023) previously detected products formed from both channels in their study of the aqueous ·OH oxidation of various GLVs. In the case of cHxO, the dominant products from the H abstraction channel were reported to be at least 15 kcal mol^{-1} more

stable than the products from the ·OH addition channel (Sarang et al., 2023). Subsequent density functional theory calculations indicated that both channels were important contributors to product formation due to the barrierless pathway in the ·OH addition channel and the formation of thermodynamically stable allylic alkyl radicals in the H abstraction channel (Sarang et al., 2023). Allylic alkyl radicals from the H abstraction channel similarly play important roles in product formation in the ·OH oxidation of large unsaturated organic compounds (Nah et al., 2014).

In contrast to cHxO, tHxO, and tPtO, the Y_{SOA} values for MBO were not statistically different ($p > 0.05$) from 0 %. The substantial differences in the Y_{SOA} values for MBO vs. cHxO, tHxO, and tPtO could be attributed to the molecular structure of MBO. MBO contains a terminal C=C bond that is adjacent to its OH group, whereas cHxO, tHxO, and tPtO contain non-terminal C=C bonds that are non-adjacent to their OH groups (Figure 1). Due to the molecular structure of MBO, the formation of RO· with oxygen radical centers adjacent to at least one OH functional group is enhanced for both the ·OH addition and H abstraction channels (Figure S9). Their close proximity to oxygenated functional groups increase the susceptibility of these RO· to fragmentation (Atkinson, 1997), which forms lower molecular weight compounds that may volatilize into the gas phase. Thus, the enhanced formation of RO· that preferentially fragment into higher volatility products during the reaction of MBO with ·OH under cloud/fog-like conditions would explain its low Y_{SOA} values. In contrast, RO· formation (and thus, fragmentation) is not enhanced in the ·OH reactions of cHxO, tHxO, and tPtO due to the formation of primary and secondary RO_2· formed from the ·OH addition and H abstraction channels.

Under the same ionic strength conditions, the Y_{SOA} values for the four GLVs were generally higher at pH 3 than at pH 5, though these pH-dependent trends were not statistically significant ($p > 0.05$) in some instances (Tables S10 to S13). It is possible that the enhanced aqSOA formation at lower pH was due to acid-catalyzed reactions. The aqueous reaction of ·OH with the four GLVs likely form various higher and lower molecular weight carbonyls (Figures S8 and S9) (Sarang et al., 2021a; Sarang et al., 2023). Some of these carbonyls could have undergone acid-catalyzed reactions (e.g., hydration, polymerization, aldol condensation) to form low volatility products (Ervens et al., 2011; Maben and Ziemann, 2023; Presberg et al., 2024; Cooke et al., 2024). Additionally, it is possible that NO· enhanced the formation of low volatility products that contributed to aqSOA at lower pH, possibly through the formation of low volatility organonitrates via the RO_2· + NO· → $RONO_2$ pathway (Atkinson and Arey, 2003). This is because NO· formation from nitrate photolysis would be enhanced at pH 3 (Table S1). HNO_2 is favored over its conjugated base NO_2^- at pH < 3.3 (Marussi and Vione, 2021). The production of NO· from the photolysis of HNO_2 (R15 in Table S1) is nearly one order of magnitude faster than its formation from NO_2^- photolysis (R10 in Table S1).

Interestingly, with the exception of cHxO at pH 3, the Y_{SOA} values for the four GLVs were higher at $I_{total} = 0.002$ M than at $I_{total} = 0.02$ M under the same pH conditions, though these ionic strength-dependent trends were not statistically significant ($p > 0.05$) in some instances (Tables S10 to S13). This is in contrast to the insignificant effect that ionic strength had on k_{obs} (Figure 2). $(NH_4)_2SO_4$ was used to control the ionic strengths of the solutions (Table 1). Thus, our results indicated

that even though ionic strength and/or sulfate concentration had insignificant effects on the reaction kinetics under cloud/fog-like conditions, they could significantly affect the formation of low volatility products. The lower Y_{SOA} values measured at higher I_{total} and sulfate concentrations under the same pH conditions implied that fragmentation reactions that form volatile lower molecular weight products were enhanced at higher I_{total} and/or sulfate concentrations. Additionally, the higher I_{total} conditions could have enhanced the partitioning of products to the gas phase due to the salting out effect (Peng and Wan, 1998).

3.2 Aqueous aerosol-like Conditions

3.2.1 Reaction Kinetics

Figure 4 shows the k_{obs} values for the four GLVs upon irradiation in the presence of nitrate at different pH (i.e., 3 vs. 5) and ionic strength (i.e., 0.5 M vs. 3.3 M). The concentrations of the GLVs and NH$_4$NO$_3$ used in this set of experiments to simulate aqueous aerosol-like conditions were both 100 times higher than those used to simulate cloud/fog-like conditions while maintaining the same nitrate/GLV molar concentration ratio of 2.5:1 (Table 1). Separate experiments performed in the absence of GLVs and using BA as the ·OH probe compound showed that the estimated [·OH]$_{ss}$ values decreased with pH under these cloud/fog-like conditions (Figure S7b), consistent with results for the cloud/fog-like conditions (Figure S7a). Unsurprisingly, the [·OH]$_{ss}$ values for aqueous aerosol-like conditions were higher than those for the cloud/fog-like conditions due to the higher concentrations of NH$_4$NO$_3$ used to simulate aqueous aerosol-like conditions. The k_{obs} values for the four GLVs were on the orders of 10^{-6} to 10^{-3} s^{-1}.
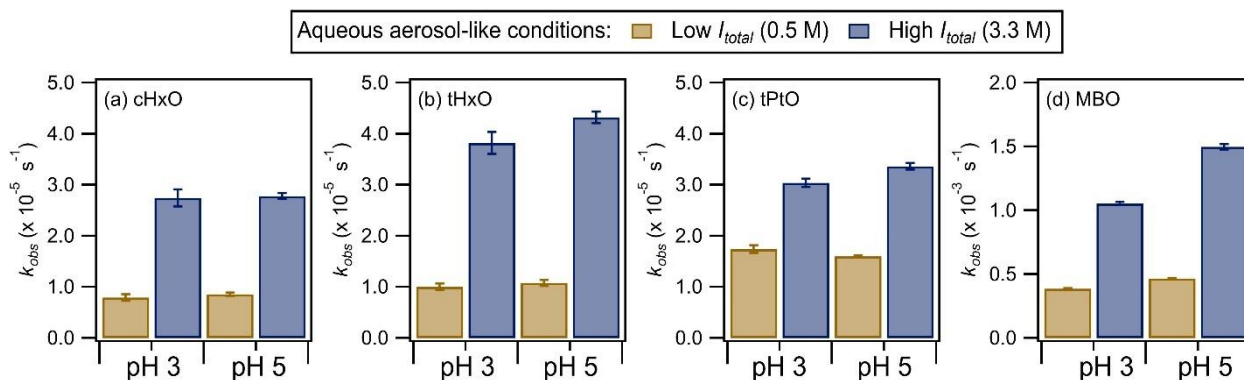
Figure 4. The k_{obs} values for the four GLVs during nitrate-mediated photooxidation under aqueous aerosol-like conditions (Table 1). The error bars represent one standard deviation originating from triplicate experiments and measurements. Statistical analyses (student's t test) on the differences in the k_{obs} values are presented in Tables S14 to S17.

The k_{obs} values measured for cHxO, tHxO, and tPtO under aqueous aerosol-like conditions were factors of 1.1 to 6.1 lower than those measured for cloud/fog-like conditions (Figure 2). The lower k_{obs} values measured for these three GLVs under aqueous aerosol-like conditions could be due, in part, to the exponential decrease in the nitrate photolysis rate with increasing

nitrate concentration (Ye et al., 2017). Consequently, the production of reactive species does not increase linearly with the nitrate concentration. Additionally, sulfur-containing radicals and reactive species produced from sulfate photolysis are expected to contribute significantly to the degradation of the GLVs under aqueous aerosol-like conditions due to the high concentration of $(NH_4)_2SO_4$ in the solutions (Cope et al., 2022). Work by Sarang et al. (2021b) suggests that the rate constants for the reactions of GLVs with $SO_4^{\cdot-}$ is about 1 order of magnitude lower than those of their reactions with $\cdot OH$ (Table S5). Nonetheless, the exponential decrease in the nitrate photolysis rate with increasing nitrate concentration does not completely explain the other noticeable differences in the k_{obs} results for aqueous aerosol-like vs. cloud/fog-like conditions. Firstly, the k_{obs} values for MBO under aqueous aerosol-like conditions were factors of 1.2 to 5.1 higher than cloud/fog-like conditions. Reasons for MBO's higher k_{obs} values under aqueous aerosol-like conditions are currently unknown. Secondly, in contrast to the insignificant effect that the ionic strength and/or sulfate concentration had on the reaction kinetics under the same pH conditions for cloud/fog-like conditions, the k_{obs} values for the four GLVs were significantly higher at $I_{total} = 3.3$ M than at $I_{total} = 0.5$ M ($p < 0.05$) under the same pH conditions for aqueous aerosol-like conditions.

The higher k_{obs} values at higher I_{total} under the same pH conditions for aqueous aerosol-like conditions could be due to higher $\cdot OH$ reactivities at higher ionic strength (Herrmann, 2003; Mekic and Gligorovski, 2021; Weller et al., 2010). Additionally, since $(NH_4)_2SO_4$ was used to control the ionic strengths of the solutions, sulfate photolysis likely contributed to the ionic strength/sulfate-dependent k_{obs} trends for the aqueous aerosol-like conditions (Table S4). Cope et al. (2022) showed that sulfur-containing radicals (e.g., $SO_4^{\cdot-}$) were formed in $(NH_4)_2SO_4$-containing concentrated solutions and aqueous aerosols when they were irradiated with UVB light or simulated sunlight. Even though the mechanism for the formation of sulfur-containing radicals from aqueous $(NH_4)_2SO_4$ photolysis remains unknown, the authors showed that the $SO_4^{\cdot-}$ formed could easily react with various organic compounds in aqueous aerosols. The $(NH_4)_2SO_4$ concentrations used in this study (0.16 M and 1.09 M) were substantially lower than the $(NH_4)_2SO_4$ concentration used by Cope et al. (2022) (3.7 M). Nevertheless, sulfate photolysis occurred under this study's aqueous aerosol-like conditions since the concentrations of the four GLVs decreased upon irradiation when only sulfate was present in the solutions (Figure S10), likely driven primarily by their reactions with $SO_4^{\cdot-}$.

Our results clearly show that sulfur-containing radicals produced from sulfate photolysis can participate in aqueous reactions with GLVs in aqueous aerosols, but not in cloud and fog droplets. This could be due to the low hydration numbers in aqueous aerosols that would reduce the energy needed to produce sulfur-containing radicals from sulfate photolysis (Cope et al., 2022; Xu et al., 1998). As explained by Cope et al. (2022), a fully-solvated SO_4^{2-} anion in dilute solutions has about 16 water molecules in its first solvation shell (Plumridge et al., 2000). The energy needed to detach an electron from $SO_4^{2-}(H_2O)_n$ to produce $SO_4^{\cdot-}(H_2O)_n$ decreases with the number of water molecules in its hydration shell, and electron detachment potentially occurs spontaneously at 3 water molecules (Pathak, 2014). Thus, the effective potential barrier for electron detachment of $SO_4^{2-}(H_2O)_4$ under concentrated conditions akin to aqueous aerosols is likely substantially lower compared to

that under dilute conditions akin to cloud and fog droplets (Yang et al., 2002). Consequently, the likelihood of sulfur-containing radical production in concentrated aqueous aerosols would be substantially higher than that in diluted cloud and fog droplets.

Comparisons of the k_{obs} values obtained in the presence of sulfate and nitrate (Figure 4) vs. only sulfate (Figure S10) indicated that sulfate photolysis had a complex non-additive effect on the GLVs' reaction kinetics. Only approximately half of the k_{obs} values measured in the presence of sulfate and nitrate were significantly higher ($p < 0.05$) than those measured in the presence of only sulfate under the same pH conditions. The non-additive effect that sulfate photolysis had on the GLVs' reaction kinetics could be due to its mechanism coupling with the nitrate photolysis mechanism. For instance, $SO_4^{\cdot-}$ could react with the NO_3^- anion to form $NO_3\cdot$ and the SO_4^{2-} anion (De Semainville et al., 2007). However, since the mechanism for the formation of sulfur-containing radicals from sulfate photolysis remains unknown, we were unable to assess the extent by which the sulfate photolysis mechanism coupled with the nitrate photolysis mechanism under our experimental conditions. Furthermore, contributions of the $\cdot OH$, $SO_4^{\cdot-}$, and $NO_3\cdot$ reactions to the measured k_{obs} would require knowledge of both the reaction rate constants and concentrations of $\cdot OH$, $SO_4^{\cdot-}$, and $NO_3\cdot$. While the $SO_4^{\cdot-}$ and $NO_3\cdot$ concentrations in our study are not known, work by Richards-Henderson et al. (2014) and Sarang et al. (2021b) suggests that the rate constants for the reactions of GLVs with $\cdot OH$, $SO_4^{\cdot-}$, and $NO_3\cdot$ are on the orders of 10^9 M^{-1} s^{-1}, 10^8 to 10^9 M^{-1} s^{-1}, and 10^7 to 10^8 M^{-1} s^{-1}, respectively (Table S5). However, the forementioned reaction rate constants were measured using dilute solutions with low ionic strengths (Sarang et al., 2021b), and it is unclear whether they could be extrapolated to aqueous aerosols which have high ionic strengths (Herrmann et al., 2015).

With the exception of tPtO at $I_{total} = 0.5$ M, the k_{obs} values were higher at pH 5 than at pH 3 under the same ionic strength conditions, though these pH-dependent trends were not statistically significant ($p > 0.05$) in some instances (Tables S14 to S17). The increase in k_{obs} with pH could potentially be due to the formation of $\cdot OH$, $SO_4^{\cdot-}$, and $NO_3\cdot$ from the coupled sulfate and nitrate photolysis mechanisms being pH-dependent, though this would require future studies to elucidate the mechanisms. The k_{obs} values measured in the presence of only sulfate did not have an obvious pH dependence (Figure S10), which could be due to the four GLVs being pH-insensitive organic compounds. Cope et al. (2022) previously reported that pH had substantial effects on the reactions of $SO_4^{\cdot-}$ with pH-sensitive organic compounds, but not on the reactions of $SO_4^{\cdot-}$ with pH-insensitive organic compounds.

3.2.2 AqSOA Mass Yields

Figure 5 shows the Y_{SOA} values for the four GLVs measured at one GLV lifetime during irradiation in the presence of nitrate at different pH (i.e., 3 vs. 5) and ionic strength (i.e., 0.5 M vs. 3.3 M). The Y_{SOA} values measured under aqueous aerosol-like conditions were substantially higher than those measured under cloud/fog-like conditions (Figure 3). The enhanced aqSOA formation under aqueous aerosol-like conditions could be attributed to the higher concentrations of GLVs, which were 100 times higher than those used under cloud/fog-like conditions. Consequently, the reaction of higher concentrations of GLVs enhanced $RO_2\cdot$ and $RO\cdot$ combination reactions that led to oligomer formation.
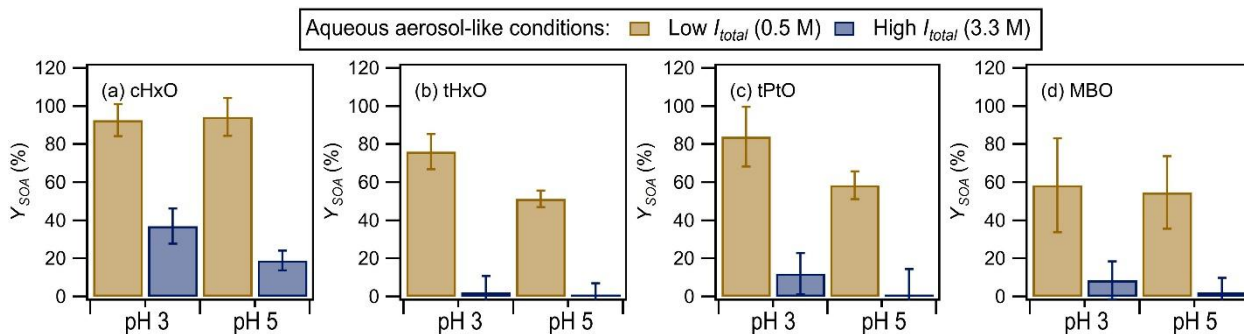
Figure 5. Y_{SOA} values for the four GLVs at one GLV lifetime during nitrate-mediated photooxidation under aqueous aerosol-like conditions (Table 1). The error bars represent one standard deviation originating from triplicate experiments and measurements, and include errors propagated from the standard deviations of the sulfate concentrations measured by ACSM. The ACSM-measured organic signals for tPtO at pH 5 at I_{total} = 3.3 M were very low, resulting in close to zero organic concentrations and Y_{SOA} values. Therefore, there was essentially no formation of low volatility products from this experiment, and the Y_{SOA} value was essentially zero. Statistical analyses (student's t test) on the differences in the Y_{SOA} values are presented in Tables S18 to S21.

Similar to the Y_{SOA} measured under cloud/fog-like conditions (Figure 3), the Y_{SOA} values for the four GLVs generally decreased with increasing pH under the same ionic strength conditions, and with increasing ionic strength and sulfate concentration under the same pH conditions, though these trends were not statistically significant ($p > 0.05$) in some instances (Tables S18 to S21). The enhanced aqSOA formation at lower pH could be due to the formation of low volatility products from acid-catalyzed reactions (e.g., hydration, polymerization, aldol condensation) (Ervens et al., 2011; Maben and Ziemann, 2023; Presberg et al., 2024; Cooke et al., 2024) and/or the enhanced formation of low volatility organonitrates via the $RO_2 \cdot$ + $NO \cdot \rightarrow RONO_2$ pathway (Atkinson and Arey, 2003). Reduced aqSOA formation at higher ionic strength and sulfate concentration was likely due to the enhancement of fragmentation pathways in the reactions of GLVs with sulfur-containing radicals formed from sulfate photolysis. For instance, $SO_4 \cdot^-$ addition to C=C bonds to form higher molecular weight organosulfates is a minor channel compared to fragmentation pathways that form lower molecular weight products induced from electron transfer and other reactions by $SO_4 \cdot^-$ (Ren et al., 2021). The higher concentrations of $SO_4 \cdot^-$ formed from the photolysis of high concentrations of sulfate ($\geq$ 1085 M) likely enhanced fragmentation pathways that led to the formation of lower molecular weight products. Additionally, the higher I_{total} conditions could have enhanced the partitioning of products to the gas phase due to the salting out effect (Peng and Wan, 1998).

Most noticeably, Y_{SOA} values as high as 59 % were measured for MBO at I_{total} = 0.5 M under aqueous aerosol-like conditions, in contrast to the substantially lower Y_{SOA} values measured under cloud/fog-like conditions ($\leq$ 9 %). While this could be due to the enhancement of $RO_2 \cdot$ and $RO \cdot$ combination reactions induced by the higher concentrations of MBO in aqueous aerosol-like conditions, the formation of low volatility organosulfates induced by reactions involving sulfate could

have contributed to the higher Y_{SOA} values as well. The concentrations of sulfate used to control the ionic strength in aqueous aerosol-like conditions were up to 1861 times higher than those used in cloud/fog-like conditions (

1). Thus, the reaction of MBO with sulfur-containing radicals formed from sulfate photolysis likely played a significant role in aqSOA formation under aqueous aerosol-like conditions. Organosulfates (e.g., 2-hydroxy-2-methyl-4sulfate-3-butanone) were previously identified as products from the reaction of MBO with $SO_4^{\cdot-}$ in the aqueous phase (Ren et al., 2021). Additionally, organosulfates could have been formed by acid-catalyzed reactions between sulfate and a MBO-derived epoxide (e.g., (3,3-dimethyloxiran-2-yl)methanol) formed from the ·OH reaction of MBO (Zhang et al., 2012). Nevertheless, increasing the sulfate concentration by 7 times to achieve $I_{total} = 3.3$ M led to substantial reductions in Y_{SOA} (9 % and 2 %). This indicated that fragmentation pathways would eventually be enhanced in the reactions of GLVs with sulfur-containing radicals formed from the photolysis of high concentrations of sulfate.

4 Conclusions and Implications

We investigated the nitrate-mediated photooxidation of four GLVs in dilute cloud/fog-like and concentrated aqueous aerosol-like conditions, focusing on the effects that pH, ionic strength, and sulfate on the reaction kinetics and aqSOA mass yields. Our results showed that the aqueous reaction medium conditions governed the effects that pH, ionic strength, and sulfate had on the reaction kinetics and aqSOA mass yields. Under dilute cloud/fog-like conditions, the four GLVs had higher k_{obs} at lower pH, which could be attributed to the pH-dependent formation of ·OH and other reactive species from nitrate photolysis. Ionic strength and sulfate had insignificant effects on k_{obs}. In contrast, under concentrated aqueous aerosol-like conditions, the four GLVs had higher k_{obs} at higher pH, as well as higher k_{obs} values at higher ionic strength and sulfate concentration. Many of these differences could be attributed to sulfur-containing radicals produced from sulfate photolysis participating in the reactions of GLVs under aqueous aerosol-like conditions, but not in cloud/fog-like conditions. Under cloud/fog-like conditions where the sulfate concentrations were low, k_{obs} was governed by the reactions of GLVs with ·OH and other reactive species from nitrate photolysis. In contrast, the high sulfate concentrations in the aqueous aerosol-like conditions enhanced the formation of sulfur-containing radicals from sulfate photolysis, which participated in the reactions of GLVs. Higher Y_{SOA} were measured under aqueous aerosol-like conditions, likely due to enhanced oligomer formation from $RO_2\cdot$ and $RO\cdot$ combination reactions caused by the higher concentrations of GLVs reacted. Despite the different effects that pH, ionic strength, and sulfate had on the reaction kinetics in cloud/fog-like vs. aqueous aerosol-like conditions, similar Y_{SOA} trends were observed for these two reaction conditions. Higher Y_{SOA} was measured at lower pH, which could be due to the enhanced formation of low volatility products from acid-catalyzed reactions and/or $RO_2\cdot + NO\cdot \rightarrow RONO_2$ reactions. Lower Y_{SOA} was measured at higher ionic strength and sulfate concentration, which could be attributed to the enhancement of fragmentation pathways in the reactions of GLVs with sulfur-containing radicals formed from sulfate photolysis.

Overall, the results provide new insights into the aqueous photooxidation of GLVs in areas with substantial levels of nitrate in cloud and fog droplets and aqueous aerosols. These insights are expected to be useful in modeling studies of the atmospheric fates of GLVs and their contributions to the SOA budget. These insights built upon those provided by previous studies that were conducted under dilute cloud/fog-like conditions and in the absence of inorganic salts (Richards-Henderson et al., 2014; Richards-Henderson et al., 2015; Sarang et al., 2021b; Sarang et al., 2023). Results from this study highlight the influences that nitrate and sulfate, the two main inorganic constituents in cloud and fog droplets and aqueous aerosols in most regions, can have on the aqueous photooxidation of GLVs. Additionally, the magnitudes of their influences depend on the aqueous reaction medium (i.e., dilute cloud and fog droplets vs. concentrated aqueous aerosols) in which the reactions occur in.

Our study also highlights many questions about the sulfate photolysis mechanism that need to be addressed in future studies. These include the mechanism for the formation of sulfur-containing radicals from aqueous $(NH_4)_2SO_4$ photolysis, and how the sulfate photolysis mechanism can couple with the nitrate photolysis mechanism to affect the formation of reactive species including $\cdot OH$. With the exception of pH 5 under aqueous aerosol-like conditions, Figure S7 showed that the $[\cdot OH]_{ss}$ generally decreased with increasing sulfate concentration, though the magnitude of the decrease depended on the pH. Additional studies are needed to elucidate how the presence of sulfate will affect the formation of reactive species under different conditions (e.g., pH, ionic strength, aqueous reaction medium). While not investigated in this study due to our inability to completely remove inorganic salts prior to UPLC-MS analysis, we hypothesize that $[\cdot OH]_{ss}$ will likely similarly decrease with increasing sulfate concentration under concentrated aqueous aerosol-like conditions. Additionally, even though this study focuses on the aqueous photooxidation of GLVs, it is likely that nitrate, sulfate, and the aqueous reaction medium will influence the aqueous photooxidation of other water-soluble organic compounds as well. More importantly, the manner in which nitrate and sulfate influence the reaction kinetics and aqSOA formation will not only depend on the aqueous reaction medium in which the reactions occur in, but also whether the water-soluble organic compound is pH-sensitive or pH-insensitive (Cope et al., 2022; Lyu et al., 2023; Yang et al., 2023). The forementioned factors need to be considered in future studies on the photooxidation of water-soluble organic compounds in different atmospheric aqueous phases.

There are several caveats that should be noted. First, we were unable to completely distinguish the effects of sulfate and ionic strength on the aqueous photooxidation of GLVs since H_2SO_4 and $(NH_4)_2SO_4$ were used to control both the pH and ionic strength of the solutions. Second, the effects of only two ionic strength conditions, 0.5 M and 3.3 M, were investigated in experiments simulating aqueous aerosols. However, ionic strengths in atmospheric aqueous aerosols span a large range and can reach 45 M (Herrmann et al., 2015; Volkamer et al., 2007). Future studies could consider using a chemically inert inorganic salt (e.g., sodium perchlorate (Mekic et al., 2018a)) to control the ionic strength of solutions and investigate reactions in aqueous aerosols with very high ionic strengths. Third, many of our conclusions regarding key reaction pathways were drawn based on Y_{SOA} measurements performed using an ACSM due to our inability to completely remove inorganic salts from experimental samples before UPLC-MS analysis. Future studies should consider using alternative analytical methods that are

not adversely impacted by inorganic salts (e.g., gas chromatography-mass spectrometry (Sarang et al., 2023) and nuclear magnetic resonance (Ren et al., 2021)) to identify prominent products and reaction pathways, though the detection of oligomers
470 is still expected to be analytically challenging.

Data availability

The data used in this publication are available to the community and can either be accessed on request to the corresponding author or online at: https://doi.org/10.5281/zenodo.14829906 (Nah et al., 2025).

Author contributions

475 YL: Conceptualization, Investigation, and Writing – original draft & editing. TJ: Investigation, Writing – review & editing. RM, MKEC, TZ, SY, CKW, and YG: Investigation. YQ: Writing – review & editing. TN: Conceptualization, Writing – review & editing, Supervision. All authors reviewed the manuscript and agreed to the final version.

Competing interests

At least one of the (co-)authors is a member of the editorial board of Atmospheric Chemistry and Physics. The authors have
480 no other competing interests to declare.

Financial support

The work described in this paper was supported by a grant from the Research Grants Council of the Hong Kong Special Administrative Region, China (project numbers 11303720 and 11303321).

References

485 Achtert, P., O'Connor, E. J., Brooks, I. M., Sotiropoulou, G., Shupe, M. D., Pospichal, B., Brooks, B. J., and Tjernström, M.: Properties of Arctic liquid and mixed-phase clouds from shipborne Cloudnet observations during ACSE 2014, Atmospheric Chemistry and Physics, 20, 14983-15002, 10.5194/acp-20-14983-2020, 2020.

Ameye, M., Allmann, S., Verwaeren, J., Smagghe, G., Haesaert, G., Schuurink, R. C., and Audenaert, K.: Green leaf volatile production by plants: a meta-analysis, New Phytol, 220, 666-683, 10.1111/nph.14671, 2018.

490 Anastasio, C. and McGregor, K. G.: Chemistry of fog waters in California's Central Valley: 1. In situ photoformation of hydroxyl radical and singlet molecular oxygen, Atmos Environ, 35, 1079-1089, 10.1016/S1352-2310(00)00281-8, 2001.

Arakaki, T., Miyake, T., Hirakawa, T., and Sakugawa, H.: pH Dependent Photoformation of Hydroxyl Radical and Absorbance of Aqueous-Phase N(III) (HNO2 and NO2-), Environ Sci Technol, 33, 2561-2565, 10.1021/es980762i, 1999.

Atkinson, R.: Atmospheric reactions of alkoxy and β-hydroxyalkoxy radicals, International Journal of Chemical Kinetics, 29,
495 99-111, 10.1002/(SICI)1097-4601(1997)29:2<99::AID-KIN3>3.0.CO;2-F, 1997.

Atkinson, R. and Arey, J.: Atmospheric degradation of volatile organic compounds, Chem Rev, 103, 4605-4638, 10.1021/cr0206420, 2003.

Benson, S. W.: Thermochemical Kinetics: Methods for the Estimation of Thermochemical Data and Rate Parameters, 2nd, Wiley1976.

500   Bianco, A., Passananti, M., Brigante, M., and Mailhot, G.: Photochemistry of the Cloud Aqueous Phase: A Review, Molecules, 25, 10.3390/molecules25020423, 2020.

Bielski, B. H. J., Cabelli, D. E., Arudi, R. L., and Ross, A. B.: Reactivity of HO2/O−2 Radicals in Aqueous Solution, Journal of Physical and Chemical Reference Data, 14, 1041-1100, 10.1063/1.555739, 1985.

Bzdek, B. R., Reid, J. P., and Cotterell, M. I.: Open questions on the physical properties of aerosols, Commun Chem, 3,
505   10.1038/s42004-020-00342-9, 2020.

Chen, G. D., Hanukovich, S., Chebeir, M., Christopher, P., and Liu, H. Z.: Nitrate Removal via a Formate Radical-Induced Photochemical Process, Environ Sci Technol, 53, 316-324, 10.1021/acs.est.8b04683, 2019.

Cofer, T. M., Engelberth, M., and Engelberth, J.: Green leaf volatiles protect maize (Zea mays) seedlings against damage from cold stress, Plant Cell Environ, 41, 1673-1682, 10.1111/pce.13204, 2018.

510   Cooke, M. E., Armstrong, N. C., Fankhauser, A. M., Chen, Y. Z., Lei, Z. Y., Zhang, Y., Ledsky, I. R., Turpin, B. J., Zhang, Z. F., Gold, A., McNeill, V. F., Surratt, J. D., and Ault, A. P.: Decreases in Epoxide-Driven Secondary Organic Aerosol Production under Highly Acidic Conditions: The Importance of Acid-Base Equilibria, Environ Sci Technol, 58, 10675-10684, 10.1021/acs.est.3c10851, 2024.

Cooper, W. J., Cramer, C. J., Martin, N. H., Mezyk, S. P., O'Shea, K. E., and von Sonntag, C.: Free Radical Mechanisms for
515   the Treatment of Methyl-Butyl Ether (MTBE) via Advanced Oxidation/Reductive Processes in Aqueous Solutions, Chem Rev, 109, 1302-1345, 10.1021/cr078024c, 2009.

Cope, J. D., Bates, K. H., Tran, L. N., Abellar, K. A., and Nguyen, T. B.: Sulfur radical formation from the tropospheric irradiation of aqueous sulfate aerosols, P Natl Acad Sci USA, 119, 10.1073/pnas.2202857119, 2022.

Daellenbach, K. R., Bozzetti, C., Krepelová, A. K., Canonaco, F., Wolf, R., Zotter, P., Fermo, P., Crippa, M., Slowik, J. G.,
520   Sosedova, Y., Zhang, Y., Huang, R. J., Poulain, L., Szidat, S., Baltensperger, U., El Haddad, I., and Prévôt, A. S. H.: Characterization and source apportionment of organic aerosol using offline aerosol mass spectrometry, Atmos Meas Tech, 9, 23-39, 10.5194/amt-9-23-2016, 2016.

de Semainville, P. G., Hoffmann, D., George, C., and Herrmann, H.: Study of nitrate radical (NO3) reactions with carbonyls and acids in aqueous solution as a function of temperature, Phys Chem Chem Phys, 9, 958-968, 10.1039/b613956f, 2007.

525   Dickson, A. G., Wesolowski, D. J., Palmer, D. A., and Mesmer, R. E.: Dissociation-Constant of Bisulfate Ion in Aqueous Sodium-Chloride Solutions to 250-Degrees-C, J Phys Chem-Us, 94, 7978-7985, DOI 10.1021/j100383a042, 1990.

Ervens, B., Turpin, B. J., and Weber, R. J.: Secondary organic aerosol formation in cloud droplets and aqueous particles (aqSOA): a review of laboratory, field and model studies, Atmospheric Chemistry and Physics, 11, 11069-11102, 10.5194/acp-11-11069-2011, 2011.

530   Ford, E., Hughes, M. N., and Wardman, P.: Kinetics of the reactions of nitrogen dioxide with glutathione, cysteine, and uric acid at physiological pH, Free Radical Bio Med, 32, 1314-1323, 10.1016/S0891-5849(02)00850-X, 2002.

García-Plazaola, J. I., Portillo-Estrada, M., Fernández-Marín, B., Kännaste, A., and Niinemets, Ü.: Emissions of carotenoid cleavage products upon heat shock and mechanical wounding from a foliose lichen, Environ Exp Bot, 133, 87-97, 10.1016/j.envexpbot.2016.10.004, 2017.

535 Gen, M. S., Liang, Z. C., Zhang, R. F., Mabato, B. R. G., and Chan, C. K.: Particulate nitrate photolysis in the atmosphere, Environ Sci-Atmos, 2, 111-127, 10.1039/d1ea00087j, 2022.

Guenther, A. B., Jiang, X., Heald, C. L., Sakulyanontvittaya, T., Duhl, T., Emmons, L. K., and Wang, X.: The Model of Emissions of Gases and Aerosols from Nature version 2.1 (MEGAN2.1): an extended and updated framework for modeling biogenic emissions, Geosci. Model Dev., 5, 1471-1492, 10.5194/gmd-5-1471-2012, 2012.

540 Hamilton, J. F., Lewis, A. C., Carey, T. J., Wenger, J. C., Borrás i Garcia, E., and Muñoz, A.: Reactive oxidation products promote secondary organic aerosol formation from green leaf volatiles, Atmospheric Chemistry and Physics, 9, 3815-3823, 10.5194/acp-9-3815-2009, 2009.

Harvey, R. M., Zahardis, J., and Petrucci, G. A.: Establishing the contribution of lawn mowing to atmospheric aerosol levels in American suburbs, Atmospheric Chemistry and Physics, 14, 797-812, 10.5194/acp-14-797-2014, 2014.

545 Heald, C. L., Collett Jr, J. L., Lee, T., Benedict, K. B., Schwandner, F. M., Li, Y., Clarisse, L., Hurtmans, D. R., Van Damme, M., Clerbaux, C., Coheur, P. F., Philip, S., Martin, R. V., and Pye, H. O. T.: Atmospheric ammonia and particulate inorganic nitrogen over the United States, Atmospheric Chemistry and Physics, 12, 10295-10312, 10.5194/acp-12-10295-2012, 2012.

Herrmann, H.: Kinetics of aqueous phase reactions relevant for atmospheric chemistry, Chem Rev, 103, 4691-4716, 10.1021/cr020658q, 2003.

550 Herrmann, H., Hoffmann, D., Schaefer, T., Bräuer, P., and Tilgner, A.: Tropospheric Aqueous-Phase Free-Radical Chemistry: Radical Sources, Spectra, Reaction Kinetics and Prediction Tools, ChemPhysChem, 11, 3796-3822, 10.1002/cphc.201000533, 2010.

Herrmann, H., Schaefer, T., Tilgner, A., Styler, S. A., Weller, C., Teich, M., and Otto, T.: Tropospheric Aqueous-Phase Chemistry: Kinetics, Mechanisms, and Its Coupling to a Changing Gas Phase, Chem Rev, 115, 4259-4334, 10.1021/cr500447k, 555 2015.

Jaoui, M., Kleindienst, T. E., Offenberg, J. H., Lewandowski, M., and Lonneman, W. A.: SOA formation from the atmospheric oxidation of 2-methyl-3-buten-2-ol and its implications for PM$_{2.5}$, Atmospheric Chemistry and Physics, 12, 2173-2188, 10.5194/acp-12-2173-2012, 2012.

Jardine, K. J., Chambers, J. Q., Holm, J., Jardine, A. B., Fontes, C. G., Zorzanelli, R. F., Meyers, K. T., De Souza, V. F., Garcia, 560 S., Gimenez, B. O., Piva, L. R. d. O., Higuchi, N., Artaxo, P., Martin, S., and Manzi, A. O.: Green Leaf Volatile Emissions during High Temperature and Drought Stress in a Central Amazon Rainforest, Plants, 4, 678-690, 2015.

Jiang, W. Q., Niedek, C., Anastasio, C., and Zhang, Q.: Photoaging of phenolic secondary organic aerosol in the aqueous phase:evolution of chemical and optical properties and effects of oxidants, Atmospheric Chemistry and Physics, 23, 7103-7120, 10.5194/acp-23-7103-2023, 2023.

565 Joo, T., Chen, Y., Xu, W., Croteau, P., Canagaratna, M. R., Gao, D., Guo, H., Saavedra, G., Kim, S. S., Sun, Y., Weber, R., Jayne, J., and Ng, N. L.: Evaluation of a New Aerosol Chemical Speciation Monitor (ACSM) System at an Urban Site in Atlanta, GA: The Use of Capture Vaporizer and PM2.5 Inlet, ACS Earth and Space Chemistry, 5, 2565-2576, 10.1021/acsearthspacechem.1c00173, 2021.

Kim, S., Rickard, C., Hernandez-Vazquez, J., and Fernandez, D.: Early Night Fog Prediction Using Liquid Water Content Measurement in the Monterey Bay Area, Atmosphere-Basel, 13, 10.3390/atmos13081332, 2022.

Korolev, A. V., Isaac, G. A., Strapp, J. W., Cober, S. G., and Barker, H. W.: measurements of liquid water content profiles in midlatitude stratiform clouds, Q J Roy Meteor Soc, 133, 1693-1699, 10.1002/qj.147, 2007.

Li, T., Wang, Z., Wang, Y. R., Wu, C., Liang, Y. H., Xia, M., Yu, C., Yun, H., Wang, W. H., Wang, Y., Guo, J., Herrmann, H., and Wang, T.: Chemical characteristics of cloud water and the impacts on aerosol properties at a subtropical mountain site in Hong Kong SAR, Atmospheric Chemistry and Physics, 20, 391-407, 10.5194/acp-20-391-2020, 2020.

Lyu, Y., Chow, J. T. C., and Nah, T.: Kinetics of the nitrate-mediated photooxidation of monocarboxylic acids in the aqueous phase, Environ Sci-Proc Imp, 25, 461-471, 10.1039/d2em00458e, 2023.

Ma, L., Guzman, C., Niedek, C., Tran, T., Zhang, Q., and Anastasio, C.: Kinetics and Mass Yields of Aqueous Secondary Organic Aerosol from Highly Substituted Phenols Reacting with a Triplet Excited State, Environ Sci Technol, 55, 5772-5781, 10.1021/acs.est.1c00575, 2021.

Maben, H. K. and Ziemann, P. J.: Kinetics of oligomer-forming reactions involving the major functional groups present in atmospheric secondary organic aerosol particles, Environ Sci-Proc Imp, 25, 214-228, 10.1039/d2em00124a, 2023.

Mack, J. and Bolton, J. R.: Photochemistry of nitrite and nitrate in aqueous solution: a review, J Photoch Photobio A, 128, 1-13, Doi 10.1016/S1010-6030(99)00155-0, 1999.

Marussi, G. and Vione, D.: Secondary Formation of Aromatic Nitroderivatives of Environmental Concern: Photonitration Processes Triggered by the Photolysis of Nitrate and Nitrite Ions in Aqueous Solution, Molecules, 26, 10.3390/molecules26092550, 2021.

Matsui, K. and Engelberth, J.: Green Leaf Volatiles—The Forefront of Plant Responses Against Biotic Attack, Plant Cell Physiol, 63, 1378-1390, 10.1093/pcp/pcac117, 2022a.

Matsui, K. and Engelberth, J.: Green Leaf Volatiles-The Forefront of Plant Responses Against Biotic Attack, Plant Cell Physiol, 63, 1378-1390, 10.1093/pcp/pcac117, 2022b.

Mekic, M. and Gligorovski, S.: Ionic strength effects on heterogeneous and multiphase chemistry: Clouds versus aerosol particles, Atmos Environ, 244, 10.1016/j.atmosenv.2020.117911, 2021.

Mekic, M., Brigante, M., Vione, D., and Gligorovski, S.: Exploring the ionic strength effects on the photochemical degradation of pyruvic acid in atmospheric deliquescent aerosol particles, Atmos Environ, 185, 237-242, 10.1016/j.atmosenv.2018.05.016, 2018a.

Mekic, M., Loisel, G., Zhou, W., Jiang, B., Vione, D., and Gligorovski, S.: Ionic-Strength Effects on the Reactive Uptake of Ozone on Aqueous Pyruvic Acid: Implications for Air–Sea Ozone Deposition, Environ Sci Technol, 52, 12306-12315, 10.1021/acs.est.8b03196, 2018b.

Mentel, T. F., Kleist, E., Andres, S., Dal Maso, M., Hohaus, T., Kiendler-Scharr, A., Rudich, Y., Springer, M., Tillmann, R., Uerlings, R., Wahner, A., and Wildt, J.: Secondary aerosol formation from stress-induced biogenic emissions and possible climate feedbacks, Atmospheric Chemistry and Physics, 13, 8755-8770, 10.5194/acp-13-8755-2013, 2013.

Nah, T., Zhang, H., Worton, D. R., Ruehl, C. R., Kirk, B. B., Goldstein, A. H., Leone, S. R., and Wilson, K. R.: Isomeric Product Detection in the Heterogeneous Reaction of Hydroxyl Radicals with Aerosol Composed of Branched and Linear

605   Unsaturated Organic Molecules, The Journal of Physical Chemistry A, 118, 11555-11571, 10.1021/jp508378z, 2014.

Nguyen, T. K. V., Zhang, Q., Jimenez, J. L., Pike, M., and Carlton, A. G.: Liquid Water: Ubiquitous Contributor to Aerosol Mass, Environ Sci Tech Let, 3, 257-263, 10.1021/acs.estlett.6b00167, 2016.

Pathak, A. K.: Conductance and bulk vertical detachment energy of hydrated sulphate and oxalate dianions: a theoretical study, Molecular Physics, 112, 1548-1552, 10.1080/00268976.2013.843035, 2014.

610   Peng, J. and Wan, A.: Effect of ionic strength on Henry's constants of volatile organic compound, Chemosphere, 36, 2731-2740, 10.1016/S0045-6535(97)10232-6, 1998.

Plumridge, T. H., Steel, G., and D. Waigh, R.: Geometry-based simulation of the hydration of small molecules, PhysChemComm, 3, 36-41, 10.1039/B003723K, 2000.

Presberg, S. S., Waters, C. M., Lyon, S. A., and Elrod, M. J.: Thermodynamics and Kinetics of Atmospherically Relevant
615   Acetalization Reactions, Acs Earth and Space Chemistry, 8, 1634-1645, 10.1021/acsearthspacechem.4c00136, 2024.

Pye, H. O. T., Nenes, A., Alexander, B., Ault, A. P., Barth, M. C., Clegg, S. L., Collett, J. L., Fahey, K. M., Hennigan, C. J., Herrmann, H., Kanakidou, M., Kelly, J. T., Ku, I. T., McNeill, V. F., Riemer, N., Schaefer, T., Shi, G. L., Tilgner, A., Walker, J. T., Wang, T., Weber, R., Xing, J., Zaveri, R. A., and Zuend, A.: The acidity of atmospheric particles and clouds, Atmospheric Chemistry and Physics, 20, 4809-4888, 10.5194/acp-20-4809-2020, 2020.

620   Ren, H., Sedlak, J. A., and Elrod, M. J.: General Mechanism for Sulfate Radical Addition to Olefinic Volatile Organic Compounds in Secondary Organic Aerosol, Environ Sci Technol, 55, 1456-1465, 10.1021/acs.est.0c05256, 2021.

Richards-Henderson, N. K., Hansel, A. K., Valsaraj, K. T., and Anastasio, C.: Aqueous oxidation of green leaf volatiles by hydroxyl radical as a source of SOA: Kinetics and SOA yields, Atmos Environ, 95, 105-112, 10.1016/j.atmosenv.2014.06.026, 2014.

625   Richards-Henderson, N. K., Pham, A. T., Kirk, B. B., and Anastasio, C.: Secondary Organic Aerosol from Aqueous Reactions of Green Leaf Volatiles with Organic Triplet Excited States and Singlet Molecular Oxygen, Environ Sci Technol, 49, 268-276, 10.1021/es503656m, 2015.

Sander, R.: Compilation of Henry's law constants (version 5.0.0) for water as solvent, Atmospheric Chemistry and Physics, 23, 10901-12440, 10.5194/acp-23-10901-2023, 2023.

630   Sarang, K., Rudzinski, K. J., and Szmigielski, R.: Green Leaf Volatiles in the Atmosphere-Properties, Transformation, and Significance, Atmosphere-Basel, 12, 10.3390/atmos12121655, 2021a.

Sarang, K., Otto, T., Rudzinski, K., Schaefer, T., Grgic, I., Nestorowicz, K., Herrmann, H., and Szmigielski, R.: Reaction Kinetics of Green Leaf Volatiles with Sulfate, Hydroxyl, and Nitrate Radicals in Tropospheric Aqueous Phase, Environ Sci Technol, 55, 13666-13676, 10.1021/acs.est.1c03276, 2021b.

635   Sarang, K., Otto, T., Gagan, S., Rudzinski, K., Schaefer, T., Brüggemann, M., Grgic, I., Kubas, A., Herrmann, H., and Szmigielski, R.: Aqueous-phase photo-oxidation of selected green leaf volatiles initiated by OH radicals: Products and atmospheric implications, Sci Total Environ, 879, 10.1016/j.scitotenv.2023.162622, 2023.

Schaap, M., van Loon, M., ten Brink, H. M., Dentener, F. J., and Builtjes, P. J. H.: Secondary inorganic aerosol simulations for Europe with special attention to nitrate, Atmospheric Chemistry and Physics, 4, 857-874, 10.5194/acp-4-857-2004, 2004.

640   Silva, D. B., Urbaneja, A., and Pérez-Hedo, M.: Response of mirid predators to synthetic herbivore-induced plant volatiles, Entomol Exp Appl, 169, 125-132, 10.1111/eea.12970, 2021.

Sindelarova, K., Granier, C., Bouarar, I., Guenther, A., Tilmes, S., Stavrakou, T., Müller, J. F., Kuhn, U., Stefani, P., and Knorr, W.: Global data set of biogenic VOC emissions calculated by the MEGAN model over the last 30 years, Atmospheric Chemistry and Physics, 14, 9317-9341, 10.5194/acp-14-9317-2014, 2014.

645   Su, Q., Yang, F., Zhang, Q., Tong, H., Hu, Y., Zhang, X., Xie, W., Wang, S., Wu, Q., and Zhang, Y.: Defence priming in tomato by the green leaf volatile (Z)-3-hexenol reduces whitefly transmission of a plant virus, Plant, Cell & Environment, 43, 2797-2811, 10.1111/pce.13885, 2020.

Tilgner, A., Schaefer, T., Alexander, B., Barth, M., Collett, J. L., Fahey, K. M., Nenes, A., Pye, H. O. T., Herrmann, H., and McNeill, V. F.: Acidity and the multiphase chemistry of atmospheric aqueous particles and clouds, Atmospheric Chemistry and 650   Physics, 21, 13483-13536, 10.5194/acp-21-13483-2021, 2021.

Volkamer, R., San Martini, F., Molina, L. T., Salcedo, D., Jimenez, J. L., and Molina, M. J.: A missing sink for gas-phase glyoxal in Mexico City: Formation of secondary organic aerosol, Geophysical Research Letters, 34, 10.1029/2007GL030752, 2007.

Weller, C., Hoffmann, D., Schaefer, T., and Herrmann, H.: Temperature and Ionic Strength Dependence of NO-radical 655   Reactions with Substituted Phenols in Aqueous Solution, Z Phys Chem, 224, 1261-1287, 10.1524/zpch.2010.6151, 2010.

West, J. J., Ansari, A. S., and Pandis, S. N.: Marginal PM(25): Nonlinear Aerosol Mass Response to Sulfate Reductions in the Eastern United States, Journal of the Air & Waste Management Association, 49, 1415-1424, 10.1080/10473289.1999.10463973, 1999.

Xu, J., Imre, D., McGraw, R., and Tang, I.: Ammonium Sulfate: Equilibrium and Metastability Phase Diagrams from 40 to 660   −50 °C, The Journal of Physical Chemistry B, 102, 7462-7469, 10.1021/jp981929x, 1998.

Xu, W., Lambe, A., Silva, P., Hu, W., Onasch, T., Williams, L., Croteau, P., Zhang, X., Renbaum-Wolff, L., Fortner, E., Jimenez, J. L., Jayne, J., Worsnop, D., and Canagaratna, M.: Laboratory evaluation of species-dependent relative ionization efficiencies in the Aerodyne Aerosol Mass Spectrometer, Aerosol Science and Technology, 52, 626-641, 10.1080/02786826.2018.1439570, 2018.

665   Yang, J., Au, W. C., Law, H., Lam, C. H., and Nah, T.: Formation and evolution of brown carbon during aqueous-phase nitrate-mediated photooxidation of guaiacol and 5-nitroguaiacol, Atmos Environ, 254, 118401, 10.1016/j.atmosenv.2021.118401, 2021.

Yang, J., Au, W. C., Law, H., Leung, C. H., Lam, C. H., and Nah, T.: pH affects the aqueous-phase nitrate-mediated photooxidation of phenolic compounds: implications for brown carbon formation and evolution, Environ Sci Process Impacts, 670   25, 176-189, 10.1039/d2em00004k, 2023.

Yang, X., Wang, X.-B., and Wang, L.-S.: Photodetachment of Hydrated Sulfate Doubly Charged Anions: $SO_4{}^{2-}(H_2O)_n$ (n = 4−40)†, The Journal of Physical Chemistry A, 106, 7607-7616, 10.1021/jp014632z, 2002.

Ye, C. X., Zhang, N., Gao, H. L., and Zhou, X. L.: Photolysis of Particulate Nitrate as a Source of HONO and NO, Environ Sci Technol, 51, 6849-6856, 10.1021/acs.est.7b00387, 2017.

675   Zhang, H. F., Worton, D. R., Lewandowski, M., Ortega, J., Rubitschun, C. L., Park, J. H., Kristensen, K., Campuzano-Jost, P., Day, D. A., Jimenez, J. L., Jaoui, M., Offenberg, J. H., Kleindienst, T. E., Gilman, J., Kuster, W. C., de Gouw, J., Park, C.,

Schade, G. W., Frossard, A. A., Russell, L., Kaser, L., Jud, W., Hansel, A., Cappellin, L., Karl, T., Glasius, M., Guenther, A., Goldstein, A. H., Seinfeld, J. H., Gold, A., Kamens, R. M., and Surratt, J. D.: Organosulfates as Tracers for Secondary Organic Aerosol (SOA) Formation from 2-Methyl-3-Buten-2-ol (MBO) in the Atmosphere, Environ Sci Technol, 46, 9437-9446, 10.1021/es301648z, 2012.

Zhang, R. F., Gen, M. S., Fu, T. M., and Chan, C. K.: Production of Formate via Oxidation of Glyoxal Promoted by Particulate Nitrate Photolysis, Environ Sci Technol, 55, 5711-5720, 10.1021/acs.est.0c08199, 2021.

Zhou, W., Mekic, M., Liu, J., Loisel, G., Jin, B., Vione, D., and Gligorovski, S.: Ionic strength effects on the photochemical degradation of acetosyringone in atmospheric deliquescent aerosol particles, Atmos Environ, 198, 83-88, 10.1016/j.atmosenv.2018.10.047, 2019.